

Nonlinearities in 20W50 and SAE 50 engine oils using low power visible laser beam

H. A. Sultan

Department of Physics, College of Education for Pure Sciences, University of Basrah, Basrah, Iraq.
hassabd67@yahoo.com

Abstract: Experimental and numerical studies of diffraction ring patterns generation in 20W50 and SAE 50 engine oils under the irradiation with visible, 473 nm, low power continuous wave laser beam are reported. The nonlinear refractive index, n_2 , for 20W50 and SAE50 are estimated to be 5.66×10^{-7} and 7.36×10^{-7} cm^2/W due to diffraction ring patterns and 1.59×10^{-9} and 2.57×10^{-9} cm^2/W due to closed aperture Z-scan technique respectively. Numerical results of the diffraction ring patterns are obtained based on Fresnel- Kirchhoff's integral.

[H. A. Sultan. **Nonlinearities in 20W50 and SAE 50 engine oils using low power visible laser beam.** *J Am Sci* 2017;13(10):20-25]. ISSN 1545-1003 (print); ISSN 2375-7264 (online). <http://www.jofamericanscience.org>. 2. doi:[10.7537/marsjas131017.02](https://doi.org/10.7537/marsjas131017.02).

Keywords: Diffraction patterns, Z-scan technique, Nonlinear refractive index, Fresnel- Kirchhoff's integral.

1. Introduction

There has been a great need for nonlinear optical materials that can be used with low-intensity lasers for optical applications such as phase conjugation, image processing, and optical storage (He, 2002-Ali and Palanisamy, 2007).

The propagation of a laser beam in a nonlinear media with intensity-dependent refractive index and absorption coefficient is accompanied by a variety of intensity phenomena. Among these are self-focusing and self-defocusing, self-phase modulation, spatial rings formation and beam breaks-up (More et al, 1988-Feit and Fleck, 1988). The spatial rings formation is based on the interference that occurs between each two points on the wavefront of the laser beam that works on the fundamental transverse mode (Durbin et al, 1981) having the same slope. The diffraction rings patterns that occurs were noticed first by Callen et al., in 1967 (Callen et al, 1967). Diffraction ring patterns (Karimzadeh, 2012) can be used to evaluate the nonlinear refractive index, n_2 . Z-scan (Shiek-Bahee et al, 1991) is another technique used to evaluate n_2 , based on the translation of a nonlinear sample through the focal point of a convergent lens.

In this article, the results of evaluating the nonlinear refractive index, n_2 , based on the diffraction ring patterns and Z-scan in 20W50 and SAE50 oils are presented. The measurements were performed using continuous wave (CW) laser beam at 473 nm wavelength.

2. Experiment

2.1 UV- visible spectroscopy

The linear absorption spectrum of 20W50 and SAE 50 oils are shown in Figure (1). The UV- visible absorption spectrum were recorded using a (Jenway-England- 6800) UV- visible spectrophotometer in the spectral range (350- 900) nm at room temperature.

The absorption coefficient, α , of 20W50 and SAE50 oils were calculated based on the absorbances (A) of 20W50 and SAE 50 oils shown in Figure (1) and the relation (Abu El-Fadl, 2012):

$$\alpha = 2.303A/d \quad (1)$$

where A is the sample absorbances and d is the sample cell thickness. Obtained absorption coefficients, α , are listed in Table (1).

2.2 Experimental setup

2.2.1 Diffraction rings experiments

To obtain the diffraction ring pattern in each sample, the experimental setup shown in Figure (2.a) comprised a CW solid state laser (SDL-473-050T) emitting light of Gaussian extent (TEM_{00} mode) of 473 nm wavelength, a 5 cm focal length positive glass lens to focus the laser light beam on each sample cell of 1mm thickness, a 30x30 cm semitransparent screen used to cast each ring pattern, a power-meter (SDL-PM-002) was used to measure the power of the laser beam falling on the samples cells and a digital camera to register each ring pattern.

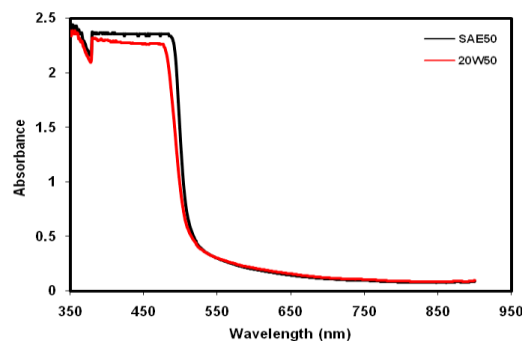


Figure 1. Linear absorbance spectrum of 20W50 and SAE 50 oils.

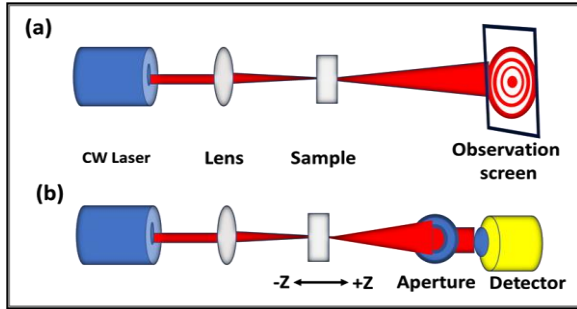


Figure 2. Experimental set-up for (a) diffraction ring patterns, (b) Z-Scan technique.

2.2.2 Z-scan experiment

The single beam closed aperture Z-Scan was carried out using the same laser considered in the previous subsection. The semitransparent screen was replaced by a photo detector with an aperture of 2.5 mm diameter fixed in front of the photo detector fed to a power meter (figure 2b.). Each sample cell was fixed on a traveling stage to scan each sample along the z-axis (direction of the laser beam propagation) passing through the positive lens focal point.

3. Results

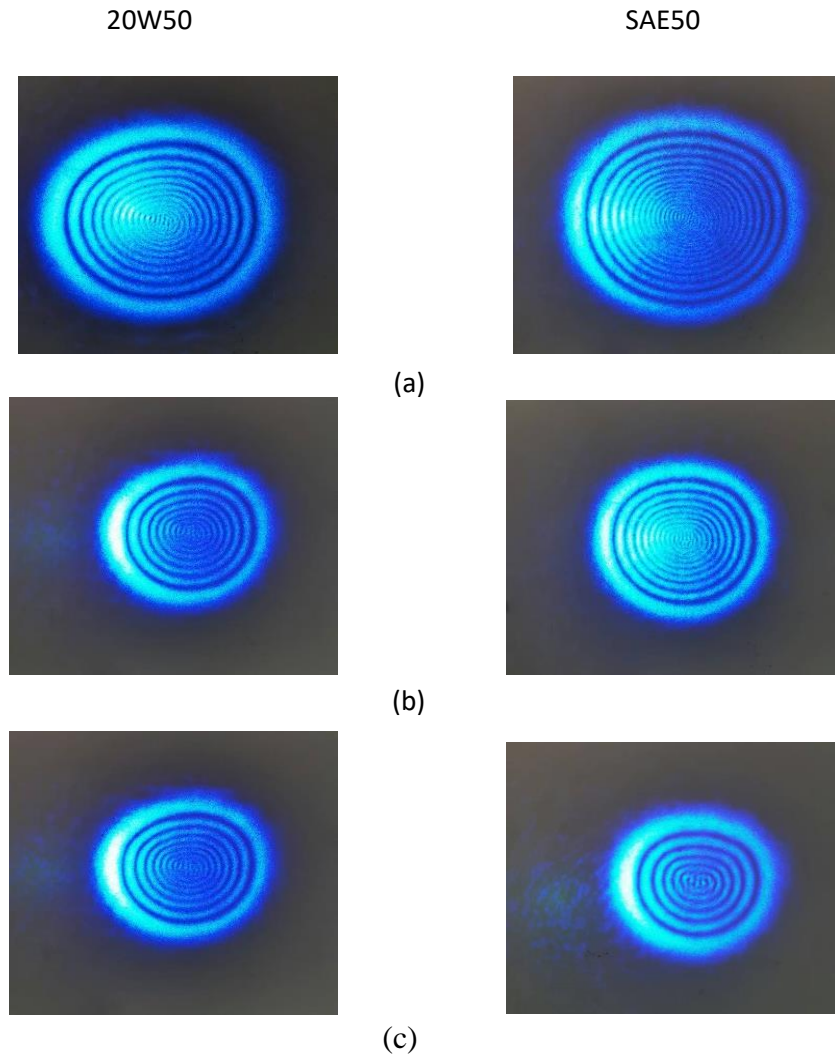


Figure (3). Diffraction ring pattern in 20W50 (left column) and SAE 50 oils (right column) at input power of (mW): (a) 48.53, (b) 37.53 and (c) 29.12.

3.1 Diffraction rings measurements

The beam radius, ω , incident on each sample cell can be obtained using the relation (Al-Ahmad et al 2013).

$$\omega = 1.22f\lambda/\omega_0 \quad (2),$$

where f is the lens focal length, ω_0 is the beam radius that fall on the lens. For $f=5$ cm, $\lambda=473$ nm and $\omega_0=1.5$ mm (at $1/e^2$), $\omega=19.235$ μm . Since the

Rayleigh length $Z_R (= \pi\omega^2/\lambda)$ (Self 1983) equals 2.46 mm in these experiments is greater than the cell thickness (1 mm), the thin sample criteria is satisfied.

Figure (3) are sample results of the diffraction ring patterns obtained for input power of (mW): (a) 48.53, (b) 37.53 and (c) 29.12.

3.2 Z-scan measurements

In the Z-scan measurements, the normalized closed aperture transmittances for both samples were measured as a function of the sample position. The laser beam ($\lambda=473$ nm) of intensity of 3.443 kW/cm² was used. Figure (4) are obtained peak to valley structures for both samples which implies negative nonlinear refractive property (self- defocusing).

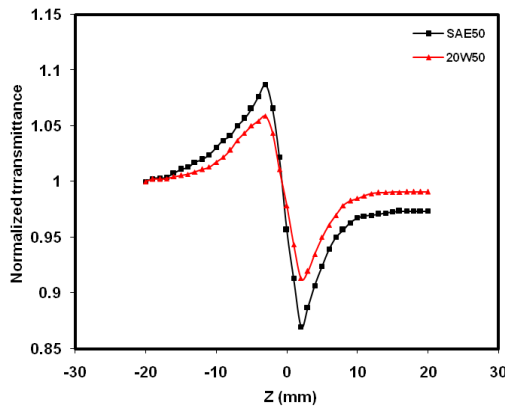


Figure 4. Closed aperture normalized Z-scan data of 20W50 and SAE 50 oils.

4. Estimation of the nonlinear refractive index of 20W50 and SAE 50 oils

4.1. When a material presents an intensity dependent refractive index it changes the beam distribution in the transverse direction of the beam propagation. According to this diffraction ring patterns appears.

Let N be the number of rings and the total phase shift, ϕ , equals to (Ogusu et al, 1996):

$$\phi = 2\pi N \quad (3)$$

The phase shift, ϕ , can be related to the path length difference, Δ , by:

$$\phi = k\Delta \quad (4)$$

The path length can be related to the change in the refractive index, Δn , each sample suffers as a result of the passage of the laser beam, by

$$\Delta = d\Delta n \quad (5),$$

where d is the sample thickness. Δn can be written as follows:

$$\Delta n = n_2 I \quad (6)$$

n_2 is the nonlinear refractive index and I is the laser beam intensity that can be written as

$$I = 2P/\pi\omega^2 \quad (7)$$

P is the input power of the laser beam and ω as defined earlier. From equations (3-6) the change in the refractive index, Δn , and the nonlinear refractive index, n_2 , can be written as:

$$\Delta n = N\lambda/d \quad (8)$$

and

$$n_2 = \Delta n/I \quad (9)$$

For the number of rings, N , appeared in each pattern given in Table (1), n_2 values are given in Table (1).

4.2. The differences between peak and valley transmittances, ΔT_{p-v} , in the Z-scan closed aperture data (Figure (4)) are related to the nonlinear refractive index, n_2 , through the relation (Cuppo et al, 2002):

$$n_2 = \Delta T_{p-v} \lambda / 4\pi d I \quad (10),$$

where all the symbols defined earlier. According to equation (10) the n_2 values are given in Table (2).

The discrepancies between diffraction ring patterns and the Z-Scan estimations of the nonlinear refractive index, n_2 , values are attributed to the use of low intensity in the later and high one in the former and since n_2 increases nonlinearly with input intensity.

Table 1: Nonlinear optical parameters for 20W50 and SAE 50 oils using diffraction rings.

Sample	Intensity W/cm ²	No. of rings N	$n_2 \times 10^{-7}$ cm ² /W
20W50	5010.16	5	4.72
	6457.54	7	5.12
	8350.27	10	5.66
SAE50	5010.16	6	5.66
	6457.54	9	6.59
	8350.27	13	7.36

Table 2: Nonlinear optical parameters for 20W50 and SAE 50 oils using Z-scan.

Sample	A cm ⁻¹	$n_2 \times 10^{-9}$ cm ² /W
20W50	52.02	1.59
SAE 50	53.82	2.37

5. Simulating the experimental diffraction ring patterns

The experimental diffraction patterns were simulated numerically by using Fresnel- Kirchhoff's theory (Majles et al, 2015) as a result of using a single transverse mode (TEM₀₀) of the irradiation laser beam.

The electric field $E(r,z)$ at the entrance of each sample cell (r is the radial coordinate) can be written as (Majles et al, 2015):

$$E(r,z) = E(0,z_0) \exp[-r^2/\omega_p^2] \exp[-ikn_0 r^2/2R] \quad (11)$$

z_0 is the medium coordinate position, k is the laser beam wave-vector of free space, n_0 is the refractive index of the medium surrounding the nonlinear material, ω_p is the beam waist at the entrance of the sample cell and R is the radius of curvature of the beam wavefront in the position. Since

the laser beam intensity traversing the sample and falling on the screen, D cm, of the sample, the light intensity, $I(\rho)$ on the screen can be calculated using the formula (Majles et al, 2015):

$$I(\rho) = I_0 \left| \int_0^{\infty} J_0(k\theta(r)) \exp[-r^2/\omega_p^2 - i\phi(r)] r dr \right|^2 \quad (12)$$

$J_0(x)$ is the zero-order Bessel function. Other symbols are defined in figure (5), and the light intensity written as

$$I_0 = 4\pi^2 [(E(0, z_0) \exp(\alpha d/2)) / i\lambda D]^2 \quad (13)$$

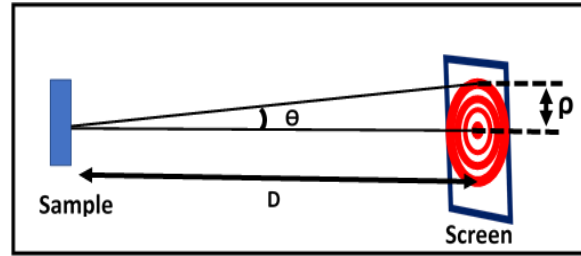


Fig.5. Definition of experimental Θ , D and ρ used in the numerical analysis of the diffraction patterns.

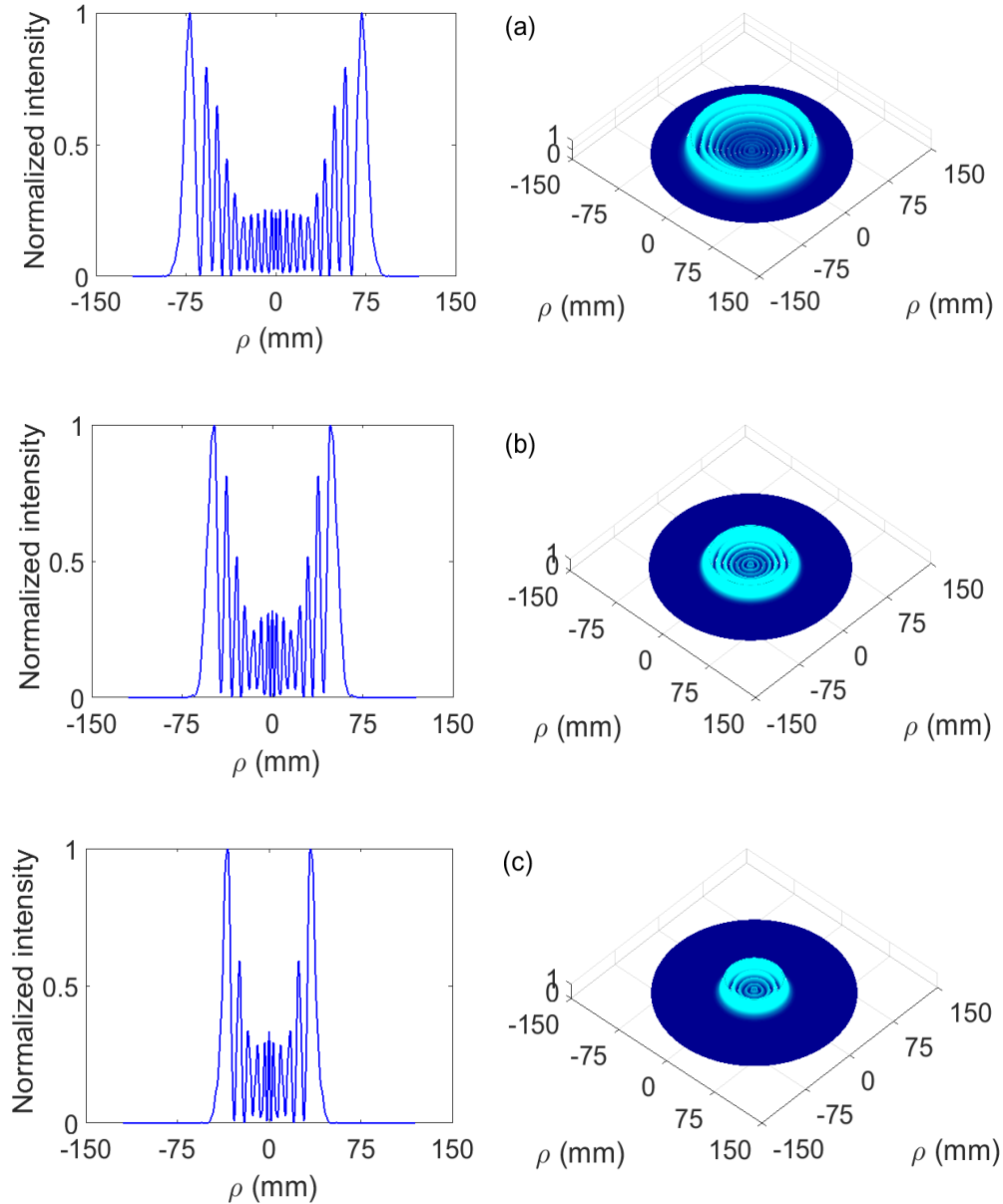


Figure (6). Intensity distribution of diffracted laser beam from 20W50 oil at powers (mW): (a) 48.53, (b) 37.53 and (c) 29.12, left and right columns are 2D and 3D distributions respectively.

Simulation results of the diffraction ring patterns are shown in figs. (6-7) for 20W50 and SAE 50 oils respectively where it can be seen that reasonable

agreement are obtained with the experimental results shown in figure (3).

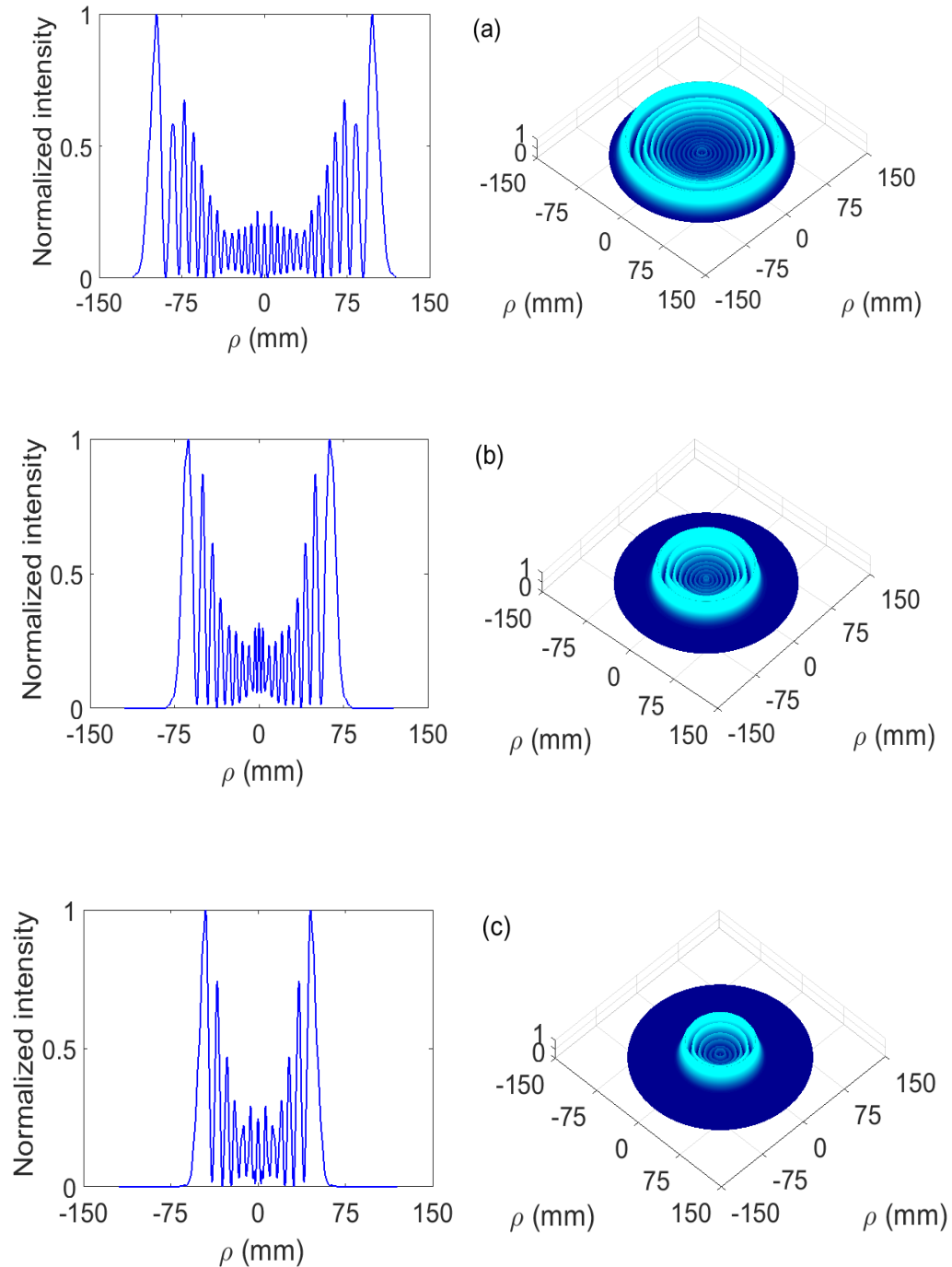


Figure (7). Intensity distribution of diffracted laser beam from SAE 50 oil at powers (mW): (a) 48.53, b) 37.53 and (c) 29.12, left and right columns are 2D and 3D distributions respectively.

6. Conclusions

The passage of a low power single transverse mode (TEM₀₀) visible laser beam results in multiple diffraction ring patterns in 20W50 and SAE50 engine oils. The diffraction patterns are calculated numerically using Fresnel- Kirchhoff's integral where good agreement obtained between experiment and numerical results. The nonlinear refractive index was calculated by the ring patterns and the closed aperture Z-scan techniques.

Acknowledgements:

Author acknowledge the fruitful discussions with professor Dr. C. A. Emshary and assist. professor Dr. Q. M. A. Hassan.

References

- G. S. He, Optical phase conjugation: principles, techniques, and applications, *Prog. Quant. Electro.* 20, 131-191 (2002).
- G. Hausler and A. Lohmann, Hybrid image processing with feedback, *Opt. Commun.* 21, 365-368 (1977).
- R.J. Longman, The next generation of 5 1/4-inch optical storage technology, *Plasmon*, Oct. (2002).
- Q. M.A. Hassan, P.K. Palanisamy, S. Manickasundaram, P. Kannan, *Opt. Sudan IV dye based poly (alkyloxymethacrylate) films for optical data storage*, *Commun.* 267, 236–243 (2006).
- S. Manickasundaram, P. Kannan, Q. M. A. Hassan, P. K. Palanisamy, Azo dye based poly (alkyloxymethacrylate)s and their spacer effect on optical data storage, *J Mater Sci: Mater Electron* 19,1045–1053 (2008).
- S. Manickasundaram, P. Kannan, R. Kumaran, R. Velu, P. Ramamurthy, Q. M. A. Hassan, P. K. Palanisamy, S. Senthil, S. Sriman Narayanan, Holographic grating studies in pendant xanthene dyes containing poly (alkyloxymethacrylate)s, *Mater Sci: Mater Electron* 22,25–34(2011).
- Q. M. Ali, P.K. Palanisamy, Optical phase conjugation by degenerate four-wave mixing in basic green 1 dye-doped gelatin film using He-Ne laser, *Optics & Laser Technology* 39, 1262–1268(2007).
- W. B. Mori, C. Joshi, J.M. Dawson, D.W. Forslund and J.M. Kindel, Evolution of self-focusing of intense electromagnetic wave in plasma, *Phys. Rev. Lett*, 60, 1298-1301 (1988).
- W.R. Callen, B.G. Huth and R.H. Pantell, Optical patterns of thermally self-defocused light, *Appl. Phys. Lett.*,11, 103-105 (1967).
- M.D. Feit and J. A. Fleck, Beam nonparaxiality, filament formation and beam breakup in the self-focusing of optical beams, *Opt. Soc. Am. B*, 5, 633-640 (1988).
- S.D. Durbin, S.M. Arakelian and Y.R. Shen, Laser-induced diffraction rings from a neurotic-liquid-crystal film, *Opt. Lett.* 6, 411-413 (1981).
- R. Karimzadeh, Spatial self-phase modulations of a laser beam propagation through liquids with self-induced natural convection flow, *J. Opt.* 14, 095701 (9pp) (2012).
- M. Sheik- Bahae, A. Said, T. -H. Wei, D.J. Haggaa, and E. W. Van Stryland, Sensitive measurement of optical nonlinearities using a single beam, *IEEE. J. Quant. Electron.* 26, 760-769 (1990).
- A. Abu El-Fadl, G. A. Mohamad, A. B. Abd El-Moiz and M. Roshad, Optical constants of Zn_{1-x}Li_xO films prepared by chemical bath deposition technique, *Physica B*, 366, 44-54 (2005).
- A. Y. Al-Ahmad, M.F. Al-Muthaffer, H. A. Badran and C. A. Emshary, Nonlinear optical and thermal properties of BCP: PMMA films determined by thermal lens diffraction, *Opt. Los. Tech.* 45, 72-78 (2013).
- S. A. Self, Focusing of spherical Gaussian beams, *Appl. Opt.* 22, 657-661 (1983).
- K. Ogusu, Y. Kohtani and H. Sao, Laser induced diffraction rings from an absorbing solution, *Opt. Rev.* 3, 232-234 (1996).
- F. L. S. Cuppo, A. M. F. Neto, S. L. Gomez and P. Palfy- Muhoray, Thermal lens model compared with the sheik- Bahae formalism in interpreting Z- Scan, experiments on lyotropic crystals, *J. Opt. Soc. Am. B*19, 1342-1348 (2002).
- M. H. Majles Ara, H. Akheratdoost and E. Koushk, Self-diffraction and high nonlinear optical properties of carbon nanotubes under cw and pulsed laser illumination, *J. Molec. Liq.*, 206, 4-9 (2015).